

Carbon Dioxide, Global Warming, and Michael Crichton’s “State of Fear”

Bert W. Rust

Mathematical and Computational Sciences Division
National Institute of Standards and Technology
100 Bureau Drive, Stop 8910
Gaithersburg, MD 20899-8910

bert.rust@nist.gov

April 13, 2006

Abstract

In his recent novel, *State of Fear* (HarperCollins, 2004), Michael Crichton questioned the connection between global warming and increasing atmospheric carbon dioxide by pointing out that for 1940-1970, temperatures were decreasing while atmospheric carbon dioxide was increasing. A reason for this contradiction was given at Interface 2003 [12] where the temperature time series was well modelled by a 64.9 year cycle superposed on an accelerating baseline. For 1940-1970, the cycle decreased more rapidly than the baseline increased. My analysis suggests that we are soon to enter another cyclic decline, but the temperature hiatus this time will be less dramatic because the baseline has accelerated. This paper demonstrates the connections between fossil fuel emissions, atmospheric carbon dioxide concentrations, and global temperatures by presenting coupled mathematical models for their measured time series.

1 Introduction

Michael Crichton’s 2004 novel *State of Fear* [1] includes scores of time series plots of surface temperatures in various parts of the world. The discussions between his characters about the significance of these plots to global warming have spilled over to the real world, inviting both praise [4, 17] and scorn [15]. In this paper, I will concentrate on one particular technical question raised early in the story. This question was introduced [1, pages 86-87] by two lawyers discussing a pending lawsuit. One of them is explaining to the other why it will be difficult to prove that increasing atmospheric carbon dioxide causes global warming. She presents her colleague with the plots reproduced in Figure 1 and asks: “*So, if rising carbon dioxide is the cause of rising temperatures, why didn’t it cause temperatures to rise from 1940 to 1970?*” There are several flaws in the plots in Figure 1, and I will correct them in the following, but the question persists even after they are corrected, so I will then answer that question, and in the process, develop mathematical models of the data that suggest that global warming is accelerating. I will also present evidence coupling that warming to global fossil fuel CO₂ emissions.

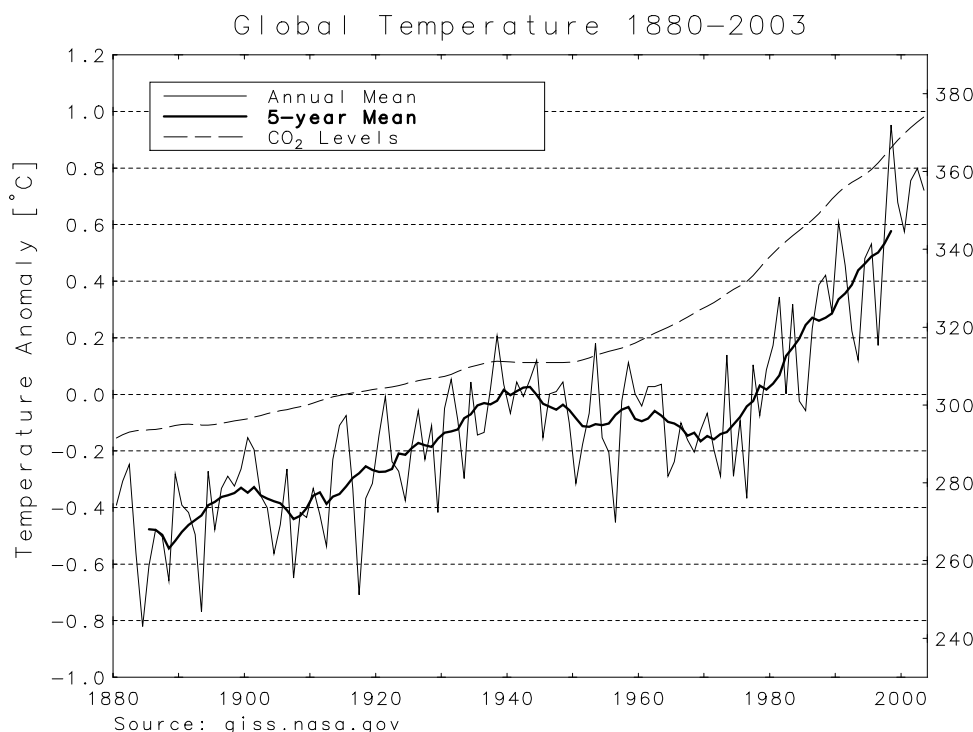


Figure 1: Michael Crichton’s plot (on page 86) of global temperatures and atmospheric CO_2 concentrations since 1880. Note that Crichton did not label the right hand axis which gives the atmospheric concentrations of CO_2 measured in parts per million by volume [ppmv]. The curve labelled “5-Year Mean” actually gives 11-year running means of the “Annual Mean” temperature anomalies.

2 Retrieving Crichton’s “Data”

The plots in Figure 1 are the best representations of the ones in the book that I was able to produce by using the Unix utility *ghostview*¹ to manually digitize the curves labelled “Annual Mean” and “ CO_2 Levels.” This exercise was necessary because Crichton’s documentation does not really identify the tabular data used to generate the two curves. A footnote on page 84 informs the reader that

All graphs are generated using tabular data from the following standard data sets: GISS (Columbia), CRU (East Anglia), GHCN and USHCN (Oak Ridge). See Appendix II for a full discussion.

Appendix II [1, pages 581-582], which has the subtitle “Sources of Data for Graphs,” informs the reader that:

World temperature data has been taken from the Goddard Institute for Space Studies, Columbia University, New York (GISS); the Jones, et al. data set from the Climate Research Unit, University of East Anglia,

¹Certain commercial equipment, instruments, or materials are identified in this paper to foster understanding. Such identification does not imply recommendation or endorsement by the National Institute of Standards and Technology, nor does it imply that the materials or equipment identified are necessarily the best available for the purpose.

Norwich, UK (CRU); and the Global Historical Climatology Network (GHCN) maintained by the National Climatic Data Center (NCDC) and the Carbon Dioxide Information and Analysis Center (CDIAC) of Oak Ridge National Laboratory, Oak Ridge, Tennessee.

It then gives the Web addresses

1. http://www.giss.nasa.gov/data/update/gistemp/station_data/
2. <http://cdiac.esd.ornl.gov/ghen/ghen.html>, and
3. <http://www.ncdc.noaa.gov/oa/climate/research/ushcn/ushcn.html>,

which lead to

1. a GISS web page from which one can retrieve surface temperatures time series from individual weather stations around the world,
2. an obsolete (no longer extant) page at the CDIAC web site, and
3. the homepage for the United States Historical Climatology Network (USHCN).

None of these pages gives the tabular data used to make the plots. The temperature time series will be considered in Section 6, but I will first develop a properly documented substitute for the curve labelled “CO₂ Levels.”

3 The “CO₂ Levels” Curve

It is clear from the context that Crichton meant for the curve to represent the atmospheric concentration of CO₂. He should have labelled the right hand vertical axis with something like “*Atm. CO₂ Conc.* [ppmv],” where [ppmv] is the abbreviation for “parts per million by volume.” Nowhere in the book did he identify the source for the plotted data. He did not even mention it in Appendix II.

Figure 2 gives a plot of the data that were probably used to construct the curve. The small solid circles (for 1959-2004) are the annual average values of the atmospheric CO₂ concentration measured by C. D. Keeling and his colleagues [7] at the Mauna Loa observatory in Hawaii. The site was chosen to give measurements that well represent globally integrated values. Several very precise measurements are made each day, so the yearly averages are highly accurate. In fact, the uncertainty intervals for the plotted averages are probably smaller than the size of the dots used to plot them.

The open squares and open diamonds are proxy measurements obtained from air bubbles trapped in the ice at two sites in Antarctica [2, 9]. They were obtained by drilling ice cores, sawing them into layers which could be dated by depth, and extracting the air from bubbles trapped in them. This trapped air was then assayed for CO₂ concentration. This method is not nearly so accurate as Keeling’s direct measurements. The estimated accuracy in dating a layer was ± 2 years. And, until the ice is sealed by compaction, the air bubbles can migrate to adjacent layers, and new air can diffuse down from the surface. So, it is necessary to correct the age of the air in each layer with a correction that depends on its depth in the ice. Thus, there is far more scatter in the ice core measurements than in the atmospheric measurements.

Crichton’s curve tracks the data in Figure 2 fairly well, but not as well as the solid curve which was obtained by fitting a mathematical model to the Mauna Loa measurements. That model depends in turn on the record of fossil fuel CO₂ emissions to the atmosphere.

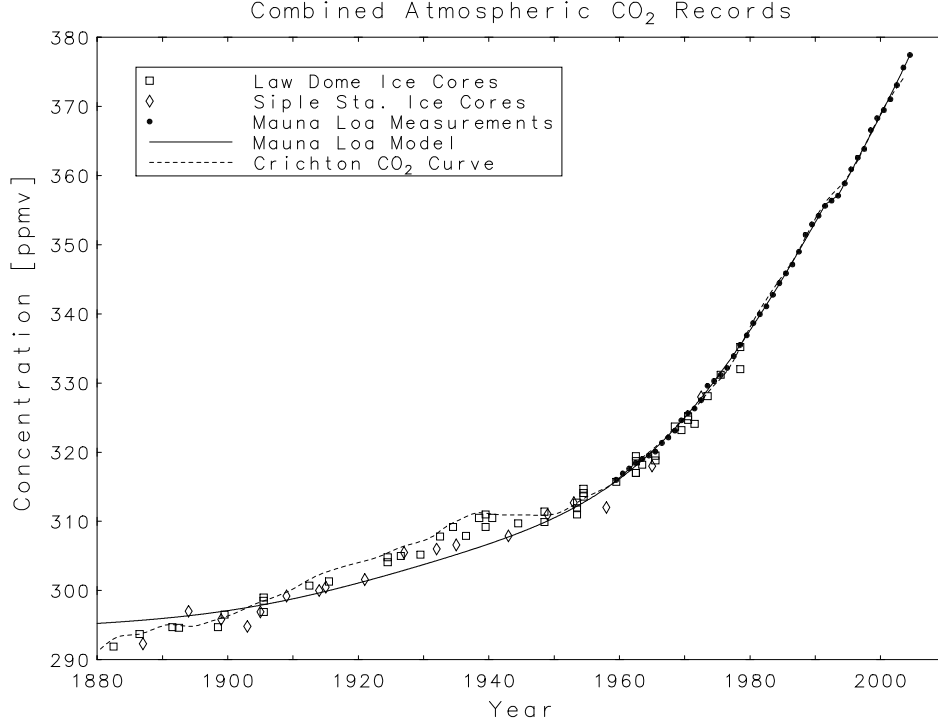


Figure 2: Comparison of Crichton’s “CO₂ Levels” curve with observed data. The plotted data can be found at:

Law Dome <http://cdiac.ornl.gov/ftp/trends/co2/lawdome.combined.dat>

Siple Sta. <http://cdiac.ornl.gov/ftp/trends/co2/siple2.013>

Mauna Loa <http://cdiac.ornl.gov/ftp/trends/co2/maunaloa.co2>

The dashed curve is Crichton’s curve from Figure 1 and the solid curve is a fit of the model (6) to the Mauna Loa measurements.

4 Fossil Fuel CO₂ Emissions

Figure 3 gives a plot of the last 147 years of the time series record of fossil fuel CO₂ emissions compiled by Marland and his colleagues [8] at the CDIAC. For all of the mathematical models and fits in the following, I will choose

$$t = 0 \quad \text{at epoch } 1856.0, \quad (1)$$

and label the time axes of the plots accordingly. Let $P(t)$ be the annual global total emissions in year t , plotted at the midpoint of each year. It was previously shown [11, 12] that $P(t)$ is well modelled by

$$P(t) = P_0 e^{\alpha t} - A_1 e^{\alpha t} \sin \left[\frac{2\pi}{\tau} (t + \phi_1) \right], \quad (2)$$

where P_0 , α , A_1 , τ , and ϕ_1 are free parameters estimated by least squares fitting. Three more years of data (2000-2002) have since been added, but the model still fits quite well. The updated parameter estimates and their standard uncertainties

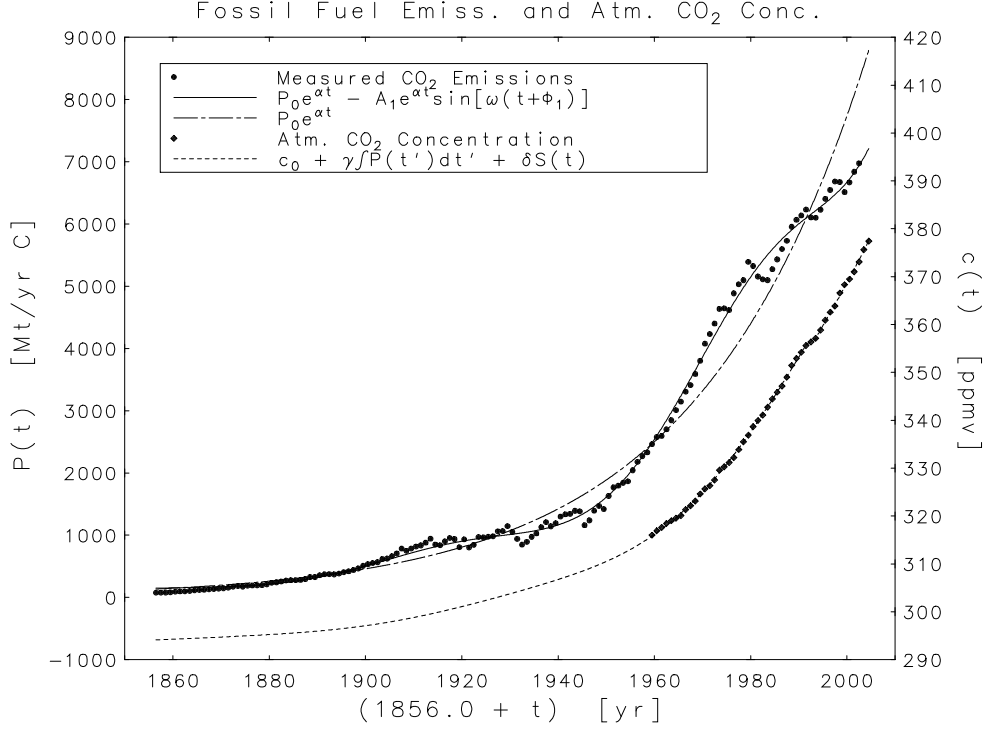


Figure 3: The discrete circles are estimated annual global totals of fossil fuel CO₂ emissions measured in millions of metric tons of carbon [Mt C]. (These data can be found at <http://cdiac.ornl.gov/ftp/ndp030/global.1751-2002.ems>.) The solid curve is the nonlinear least squares fit of the model (2), and the dot-dashed curve is the exponential baseline obtained in that fit. The discrete diamonds are Keeling's Mauna Loa measurements of the atmospheric CO₂ concentration. The dashed curve is the fit of the model (6) to Keeling's data.

are

$$\begin{aligned} \hat{P}_0 &= 132.7 \pm 4.4 \text{ [Mt/yr C]}, & \hat{A}_1 &= 25.1 \pm 1.1 \text{ [Mt/yr C]}, \\ \hat{\alpha} &= 0.02824 \pm .00029 \text{ [yr}^{-1}\text{]}, & \hat{\tau} &= 64.7 \pm 1.4 \text{ [yr]}, \\ & & \hat{\phi}_1 &= -6.1 \pm 2.4 \text{ [yr]}, \end{aligned} \quad (3)$$

and the model explains 99.76 % of the variance in the record.

The model is a sum of an exponential baseline, plotted as a dashed curve, and an ≈ 65 year sinusoidal oscillation whose amplitude grows with the same exponential rate as the baseline. Biological processes are often exponential, so the baseline is not surprising, but the oscillation is remarkable. Its magnitude exceeds that of the largest manmade perturbations like the Great Depression, World War II, the OPEC oil embargo, and the 1980s “energy crisis,” all of which are clearly visible in the data. Note that the oscillating term is preceded by a minus sign. We shall see, in Section 7, that an oscillation with the same period and phase shift occurs in the global temperature record, but there it is preceded by positive sign. This suggests a negative temperature feedback in fossil fuel production.

It will be convenient in the following to introduce the angular frequency

$$\omega \equiv \frac{2\pi}{\tau}, \quad \hat{\omega} = 0.0971 \text{ [rad/yr]}, \quad (4)$$

which allows the model (2) to be written

$$P(t) = P_0 e^{\alpha t} - A_1 e^{\alpha t} \sin [\omega(t + \phi_1)] . \quad (5)$$

5 A Model for Atmospheric CO₂

The solid curve in Figure 2 and the dashed curve in Figure 3 are two different plots of the same three parameter, linear least squares fit to Keeling's Mauna Loa measurements. For any given t , the fitted model can be written

$$c(t) = c_0 + \gamma \int_0^t P(t') dt' + \delta S(t) , \quad (6)$$

where c_0 , γ , and δ are the free parameters, $P(t')$ is defined by Equation (2) or (5), using the estimates (3), and $S(t)$ is a linear ramp function which models the perturbation, clearly visible in the data, caused by the Mount Pinatubo eruption in June 1991. More precisely,

$$S(t) \equiv \begin{cases} 0 , & t \leq t_P \\ \frac{1}{2}(t - t_P) , & t_P < t < (t_P + 2) \\ 1 , & (t_P + 2) \leq t \end{cases} \quad (7)$$

where

$$t_P = 1991.54 - 1856.0 = 135.54 . \quad (8)$$

The parameter c_0 represents the atmospheric CO₂ concentration at epoch 1856.0. The integral, for any time t , represents the cumulative emissions from 1856.0 until $(1856.0 + t)$, and the parameter γ gives the fraction of those emissions which remains in the atmosphere. The function $S(t)$ represents a linear increase of one unit spread over two years following the initial eruption, so the parameter δ represents the amplitude of the perturbation. The $S(t)$ term is preceded by a positive sign in the model, but the estimate $\hat{\delta}$ turned out to be negative, so the volcano caused a small reduction in atmospheric CO₂. The reason, according to Gu, et. al. [3] was enhanced terrestrial photosynthesis caused by an aerosol-induced increase in diffuse radiation.

Using the parameter estimates (3) and (4) in Equation (5) gives

$$\int_0^t P(t') dt' = \int_0^t \left\{ \hat{P}_0 e^{\hat{\alpha} t'} - \hat{A}_1 e^{\hat{\alpha} t'} \sin [\hat{\omega}(t' + \hat{\phi}_1)] \right\} dt' \quad (9)$$

$$= \hat{Q}_2 + \hat{R}_2 e^{\hat{\alpha} t} - \hat{A}_2 e^{\hat{\alpha} t} \sin [\hat{\omega}(t + \hat{\phi}_2)] , \quad (10)$$

where

$$\begin{aligned} \hat{Q}_2 &\equiv \left[\frac{\hat{A}_1 \hat{\alpha} \sin(\hat{\omega} \hat{\phi}_1) - \hat{A}_1 \hat{\omega} \cos(\hat{\omega} \hat{\phi}_1)}{\hat{\alpha}^2 + \hat{\omega}^2} - \frac{\hat{P}_0}{\hat{\alpha}} \right] = -4930 \text{ [Mt C]} , \\ \hat{R}_2 &\equiv \frac{\hat{P}_0}{\hat{\alpha}} = 4700 \text{ [Mt C]} , \\ \hat{\phi}_2 &\equiv \frac{1}{\hat{\omega}} \tan^{-1} \left[\frac{\hat{\alpha} \sin(\hat{\omega} \hat{\phi}_1) - \hat{\omega} \cos(\hat{\omega} \hat{\phi}_1)}{\hat{\alpha} \cos(\hat{\omega} \hat{\phi}_1) + \hat{\omega} \sin(\hat{\omega} \hat{\phi}_1)} \right] = -19.3 \text{ [yr]} , \\ \hat{A}_2 &\equiv \frac{\hat{A}_1}{\sqrt{\hat{\alpha}^2 + \hat{\omega}^2}} = 248 \text{ [Mt C]} . \end{aligned} \quad (11)$$

The model (6) can thus be written

$$c(t) = c_0 + \gamma \left\{ \hat{Q}_2 + \hat{R}_2 e^{\hat{\alpha}t} - \hat{A}_2 e^{\hat{\alpha}t} \sin \left[\hat{\omega}(t + \hat{\phi}_2) \right] \right\} + \delta S(t) , \quad (12)$$

with only c_0 , γ , and δ unknown. To fit this to Keeling's data, we must change the units in (11) from [Mt C] to [ppmv]. The conversion factor given by Watts [16] is

$$1 \text{ [ppmv]} = 2130 \text{ [Mt C]} , \quad (13)$$

so

$$\hat{Q}_2 = -2.32 \text{ [ppmv]} , \quad \hat{R}_2 = 2.21 \text{ [ppmv]} , \quad \hat{A}_2 = 0.116 \text{ [ppmv]} . \quad (14)$$

Using these values to fit Equation (12) to the Mauna Loa data yields the estimates

$$\hat{c}_0 = 294.10 \pm .19 \text{ [ppmv]} , \quad \hat{\gamma} = 0.5926 \pm .0026 , \quad \hat{\delta} = -2.05 \pm .20 \text{ [ppmv]} , \quad (15)$$

and the solid curve in Figure 2. The fit, which explains 99.97 % of the variance in the record, is better than it looks in that figure which is cluttered with other information. Cleaner plots are given in Figures 3 and 5. If the ice core proxy data are included in the fit, the resulting curve is not much changed, but the residuals for 1959-2003 are noticeably degraded. So it seems better to back-extrapolate the very good fit to the very good data than to use the degraded fit to the combined data set.

6 Crichton's Temperature Anomaly Data

The term *temperature anomaly* can be defined by the equation

$$\left[\begin{array}{c} \text{Temp. "anomaly"} \\ \text{for year } t_i \end{array} \right] \equiv \left[\begin{array}{c} \text{Average Temp.} \\ \text{in year } t_i \end{array} \right] - \left[\begin{array}{c} \text{Average Temp. for} \\ \text{some reference period} \end{array} \right] . \quad (16)$$

The quantity of interest in global warming studies is temperature change, so it does not matter where the zero point is chosen. Absolute temperatures can be recovered from the anomalies by adding the reference temperature. Two anomaly records using different reference temperatures can be brought into concordance by shifting one of them to make its average value agree with that of the other.

The note "Source: giss.nasa.gov" at the lower left of Crichton's plot (Figure 1) suggests that he obtained his data from the Goddard Institute for Space Studies (GISS) web-site. Goddard maintains two records of global annual average temperature anomalies which can be found at

<http://data.giss.nasa.gov/gistemp/taledata/GLB.Ts.txt> , and

<http://data.giss.nasa.gov/gistemp/taledata/GLB.Ts+dSST.txt> .

The first is based on the data from meteorological stations, and the second on land plus ocean temperatures. Neither matches Crichton's plot. The GISS land + ocean anomalies are plotted together with Crichton's curve in Figure 4 which also includes a plot of the global annual average anomalies maintained by the University of East Anglia's Climatic Research Unit (CRU) at

<http://www.cru.uea.ac.uk/cru/data/temperature/> .

The GISS and CRU anomalies are consistent with one another, but the Crichton values differ significantly from them. In the midrange 1910-1980, all three records vary in concert, but the Crichton values display more pronounced extremes than the other two records. This suggests that less averaging was used in computing

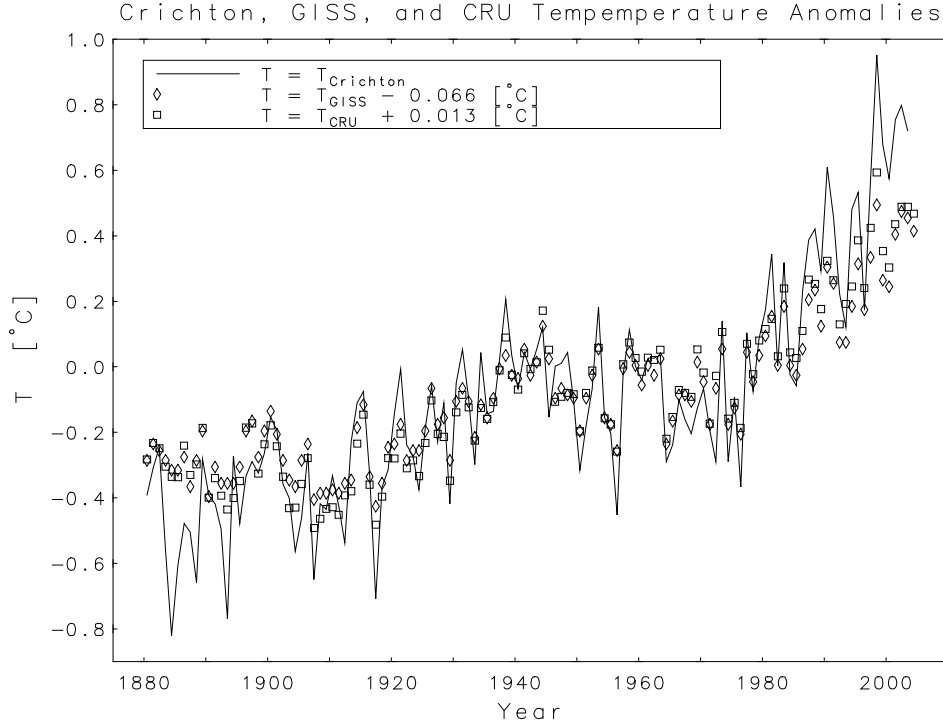


Figure 4: The jagged curve is Crichton's record from Figure 1. The diamonds are the GISS land + ocean anomalies adjusted to have the same average value as the Crichton record. The squares are the similarly adjusted CRU global averages.

them. In the beginning range 1880-1910, the Crichton values are significantly lower than the other two records, and in the end range 1980-2003, they are significantly higher. Thus, the Crichton record indicates a greater total warming over the range 1880-2003 than do the GISS and CRU records. Similar results are obtained by comparing the Crichton record with the GISS meteorological station record and with the USHCN record. Since it is not clear how or where he got his data, I have used the CRU record to make a reconstruction of Figure 1 which is given here in Figure 5. This reconstruction does not obviate the question of why temperatures fell during the period 1940-1970, but it does show a similar cooling during the years 1880-1910. This cooling is clearly visible also in both the CRU and GISS plots in Figure 4 but not in Crichton's record.

7 The 65 Year Cycle in Global Temperatures

The answer to Crichton's question is that global temperatures oscillate around an increasing baseline with a period of ≈ 65 years. This oscillation, and its obscuration of the global warming signal, was first described by Schlesinger and Ramankutty [14] who also suggested that it "arises from predictable internal variability of the ocean-atmosphere system." It is clearly visible in the 11-year running mean curve plotted in Figure 5. Figure 6 gives plots of 4 different linear least squares fits to the CRU global average temperature anomalies. For each fit, the model had the form

$$T(t) = (\text{increasing baseline}) + (64.7 \text{ year cycle}) . \quad (17)$$

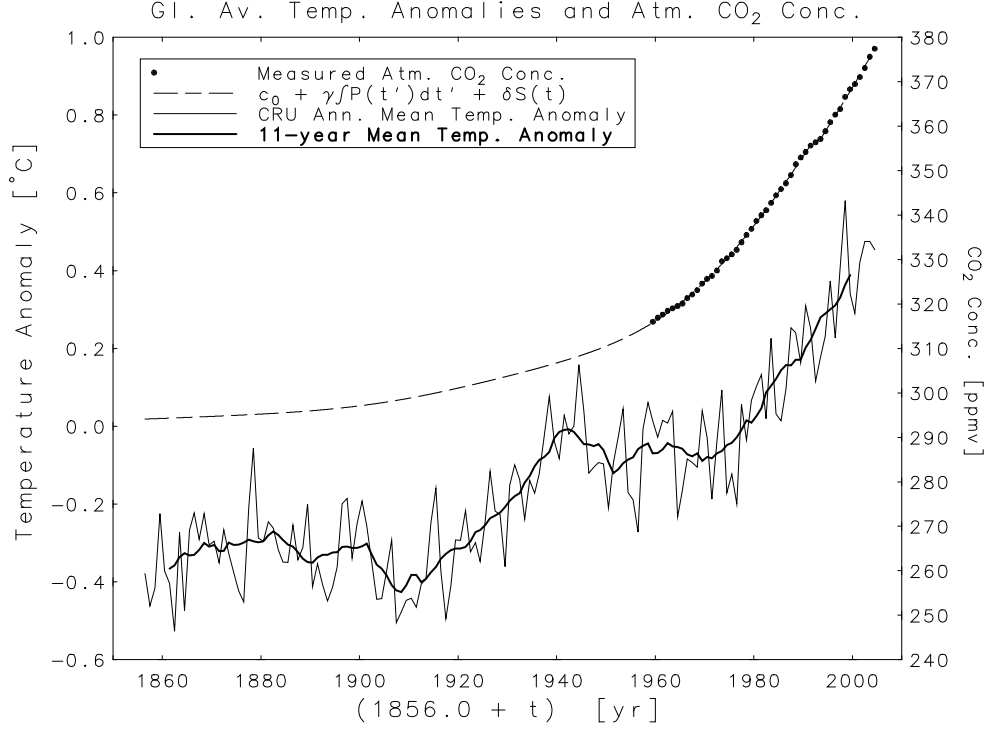


Figure 5: Improved and corrected versions of Crichton's plots in Figure 1. The construction of the CO_2 concentration curve is described in Section 5. The temperature curve is the CRU time series which was chosen because it is the longest record available and because it was used in previous studies that will be cited here. The reference period used in defining the temperature anomalies was 1961-1990.

More precisely, the four models were

$$T(t) = T_0 + \eta t + A_3 \sin [\hat{\omega}(t + \hat{\phi}_1)] , \quad (18)$$

$$T(t) = T_0 + \eta t^2 + A_3 \sin [\hat{\omega}(t + \hat{\phi}_1)] , \quad (19)$$

$$T(t) = T_0 + \eta \exp\left(\frac{3\hat{\alpha}}{5}t\right) + A_3 \sin [\hat{\omega}(t + \hat{\phi}_1)] , \quad (20)$$

$$T(t) = T_0 + \eta [\hat{c}(t) - \hat{c}_0]^{2/3} + A_3 \sin [\hat{\omega}(t + \hat{\phi}_1)] , \quad (21)$$

where T_0 , η , and A_3 are the free parameters. The frequency $\hat{\omega}$, given by Equation (4), is the same as that of the oscillation in the fossil fuel emissions model (5) which, by (3), corresponds to a period $\hat{\tau} = 64.7$ [yr]. The phase shift $\hat{\phi}_1$ is also the same as the one given in (3) for the emissions model. But here the oscillating term is preceded by a plus sign, so maxima in the temperature cycle correspond to minima in the emissions cycle, and vice versa. This inverse correlation between the variations in the two time series was first pointed out in 1982 by Rust and Kirk [13] who noted that those variations “appear to follow a quasicycle.” They attributed the inverse correlation to a temperature dependent modulation of the exponential

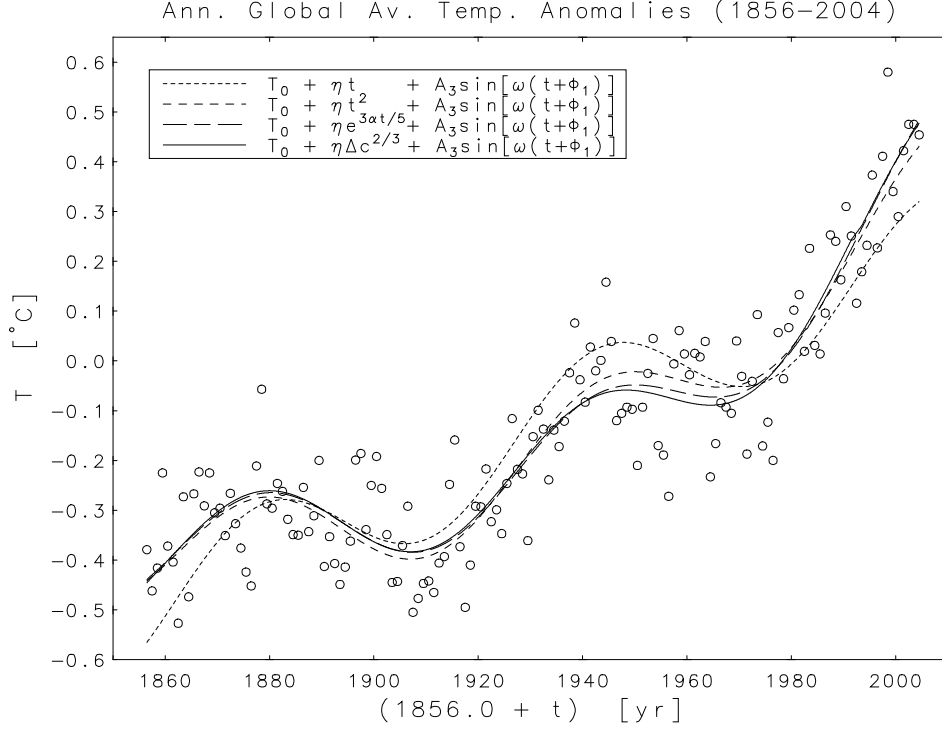


Figure 6: The open circles are the CRU global average temperature anomalies. The 4 curves are three-parameter, linear least squares fits of the four models (18) - (21). The $\Delta c^{2/3}$ in the last line of the legend is an abbreviation for $[\hat{c}(t) - \hat{c}_0]^{2/3}$.

growth rate in fossil fuel production and modelled it with the simple ODE

$$\frac{dP}{dt} = \left(\alpha - \beta \frac{dT}{dt} \right) P, \quad P(0) = P_0 \quad (22)$$

with free parameters α , P_0 , and β . The α and P_0 are analogous to their counterparts in (2), and β expresses the strength of the modulation. Using the crude temperature record available at the time, they got a good fit to the emissions time series.

8 The Accelerating Baseline

The parameter estimates and some residual diagnostics produced by the four fits are given in Table 1. It is clear from the diagnostics, and from the curves plotted in Figure 6, that the linear baseline model (18) does not fit the data nearly so well as the other three. The inadequacy of a linear baseline has previously been demonstrated in [10, 11, 12]. The residuals for the fit, plotted in Figure 7, display a pronounced concave upward pattern not shared by those of the other models. Clearly, *the data demand an accelerating baseline*.

The quadratic baseline in (19) produces warming with a constant acceleration $2\hat{\eta} = 6.58 \times 10^{-5} \text{ } [^{\circ}\text{C}/\text{yr}^2]$. It was shown in [10, 12] that adding a linear term to the quadratic model does not produce a statistically significant reduction in the SSR. For the updated temperatures used here, including a linear term gives $\text{SSR} = 1.2697$. The standard F-test shows that this is not a statistically significant improvement

Table 1: Parameter estimates and residual diagnostics for the models (18) - (21). The uncertainties in the estimates are the estimated standard deviations. The value SSR is the sum of squared residuals for the fit, and R^2 is the coefficient of determination, so $100R^2$ gives the percentage of the total variance that is explained by the model.

Param.	$T_0 + \eta t$ baseline	$T_0 + \eta t^2$ baseline	$T_0 + \eta e^{3\hat{\alpha}t/5}$ baseline	$T_0 + \eta(\Delta c)^{2/3}$ baseline
\hat{T}_0	$-0.510 \pm .019$	$-0.390 \pm .012$	$-0.460 \pm .013$	$-0.400 \pm .012$
$\hat{\eta}$	$(4.87 \pm .22) \times 10^{-3}$	$(3.29 \pm .12) \times 10^{-5}$	$0.0690 \pm .0024$	$(2.490 \pm .087) \times 10^{-4}$
\hat{A}_3	$0.112 \pm .014$	$0.100 \pm .011$	$0.093 \pm .011$	$0.095 \pm .011$
SSR	1.8965	1.2891	1.2604	1.2630
$100R^2$	77.91 %	84.99 %	85.32 %	85.29 %

over $SSR = 1.2891$. Thus *the data since 1856.0 demand a monotonically increasing baseline.*

The rate constant chosen for the exponential baseline in (20) was $3\hat{\alpha}/5 = 0.01694 \text{ [yr}^{-1}]$ where $\hat{\alpha}$ is the fossil fuel rate constant given by Equation (3). It produces a monotonically increasing, accelerated warming, but it does not establish a strong connection between the warming and the fossil fuel emissions. A wide range of other choices would work just as well. If the rate constant is allowed to be a free parameter also, i.e., if

$$T(t) = T_0 + \eta \exp(\alpha' t) + A_3 \sin[\hat{\omega}(t + \hat{\phi}_1)] , \quad (23)$$

then the resulting estimates $\hat{\eta} = 0.071 \pm .024$ and $\hat{\alpha}' = 0.0168 \pm .0022$ have a correlation coefficient $\hat{\rho}(\eta, \alpha') = -0.995$. This strong inverse correlation indicates that the data cannot uniquely determine both parameters and that many combinations of the two would give approximately the same fit. Similar results would be obtained by fixing α' at any of the values in the standard uncertainty interval $0.0146 \leq \alpha' \leq 0.0190$. Thus, *although the data demand an accelerating baseline, they are not yet extensive enough to precisely determine the rate of acceleration.*

The most interesting of the four models is (21) because its baseline is based on a power law relation between changes in temperature and changes in the atmospheric CO_2 concentration. If one assumes a baseline variation law of the form

$$[T(t) - T_0] = \eta [c(t) - c_0]^\nu , \quad (24)$$

with a new free parameter ν , then adding the 65 year cycle to the model gives

$$T(t) = T_0 + \eta [\hat{c}(t) - \hat{c}_0]^\nu + A_3 \sin[\hat{\omega}(t + \hat{\phi}_1)] , \quad (25)$$

where $\hat{c}(t)$ is calculated by substituting the estimates in Equation (15) into the model defined by Equation (12). Fitting this model gives a curve which is almost identical to the one obtained by fitting (21), i.e., the one plotted as a solid curve

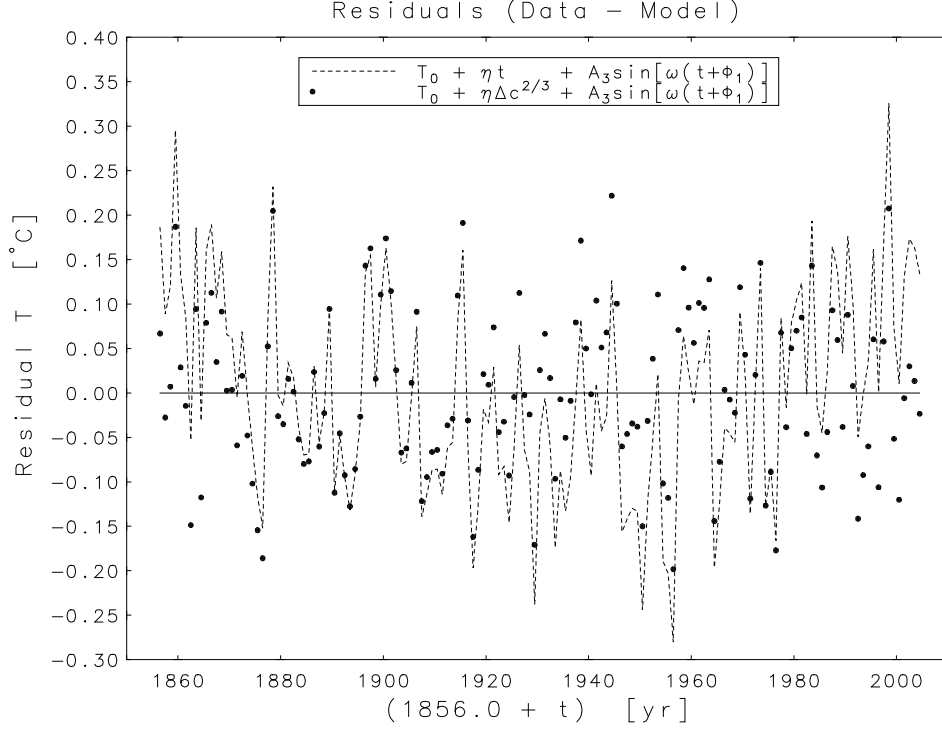


Figure 7: The residuals (data - model) for the fits of models (18) and (21). The residuals for models (19) and (20), which were very similar to those for (21), were not plotted in order to reduce clutter.

in Figure 6. But the estimates $\hat{\eta} = (3.2 \pm 2.5) \times 10^{-4}$ and $\hat{\nu} = 0.645 \pm .063$ have a correlation coefficient $\hat{\rho}(\eta, \nu) = -0.9989$, so the data cannot support unique estimates of both parameters. Therefore, I chose to fix the value $\nu = 2/3$ because it is a simple rational number close to the middle of the standard uncertainty interval $0.582 \leq \nu \leq 0.708$.

The power law model does not fit the data significantly better than the quadratic or exponential baseline models, but it relates the warming directly to the fossil fuel emissions through the 3 equations:

$$P(t) = P_0 e^{\alpha t} - A_1 e^{\alpha t} \sin \left[\frac{2\pi}{\tau} (t + \phi_1) \right], \quad (26)$$

$$c(t) = c_0 + \gamma \int_0^t P(t') dt' + \delta S(t), \quad (27)$$

$$T(t) = T_0 + \eta [c(t) - c_0]^{2/3} + A_3 \sin \left[\frac{2\pi}{\tau} (t + \phi_1) \right]. \quad (28)$$

And the perfect negative correlation between the oscillations in the first and last of these suggests the possibility of expressing $P(t)$ in terms of $T(t)$ in a feedback model, perhaps similar to Equation (22), in which the increasing temperatures limit the fossil fuel emissions.

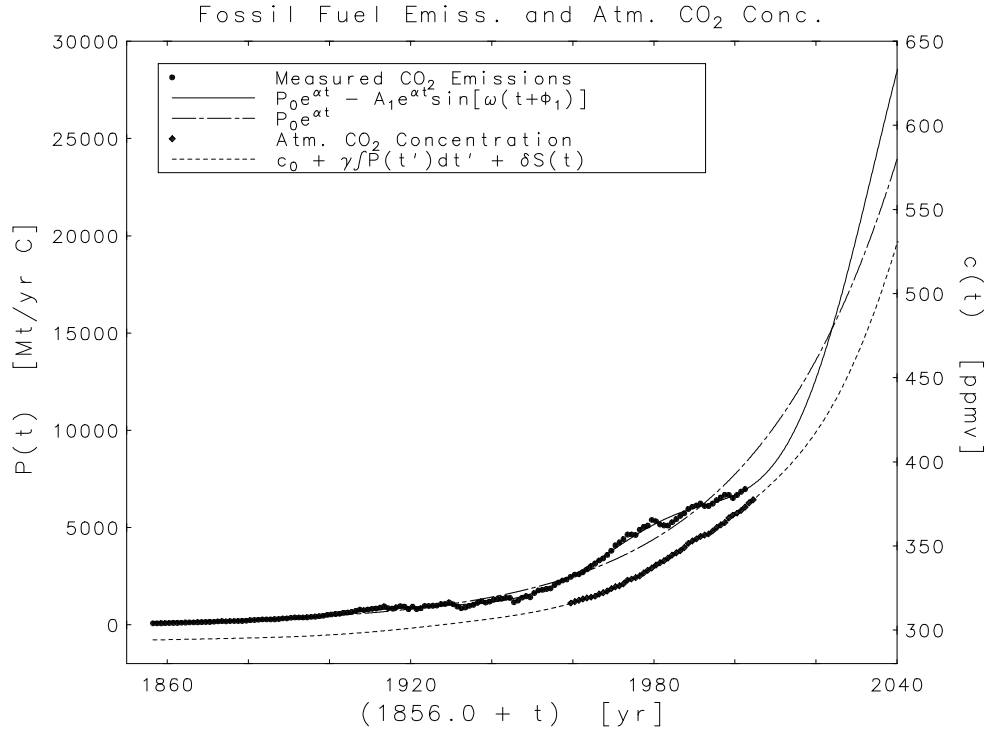


Figure 8: Extrapolated fossil fuel emissions and the resulting atmospheric CO₂ concentrations

9 Extrapolating into the Future

If the rising temperatures do not limit fossil fuel emission rates, then they will eventually be limited by the exhaustion of the world's fossil fuel reserves. Although the model (2) fits the data quite well thus far, that sort of exponential behaviour cannot be continued indefinitely. Using the estimates in Equation (3) to extrapolate to epoch 2100.0 yields a fossil fuel emissions rate of $\approx 140,000$ [Mt/yr C] which is ≈ 20 times greater than the present rate. This seems rather implausible, but coal reserves are quite large and new technologies for burning coal cleanly are being developed quite rapidly, so it might be possible to continue the present behaviour for another half cycle of the sinusoidal oscillation. The next maximum of the temperature cycle will occur in September 2007. The next minimum will then occur in March 2040. Figure 8 shows the extrapolations given by equations (2) and (6). If such emission rates are sustainable, then the corresponding temperature extrapolations are given in Figure 9. Only the constant acceleration, quadratic baseline model produces a noticeable hiatus in the rising temperature.

Acknowledgements

I would like to thank Dr. David Kahaner for bringing *State of Fear* to my attention and suggesting that I write this paper. I would also like to thank Drs. Ronald Boisvert, Timothy Burns and Adriana Hornikova for their suggestions for improving the manuscript.

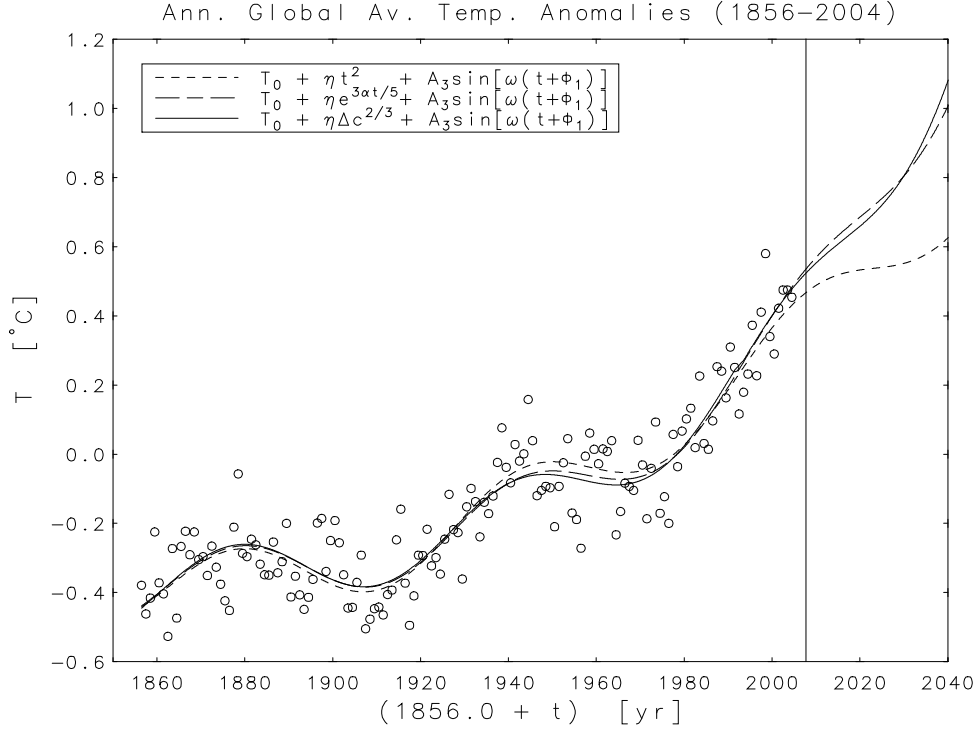


Figure 9: Extrapolations of the temperature models (19), (20), and (21). The vertical line in the year 2007 marks the beginning of the next cooling segment of the 65 year cycle.

References

- [1] Crichton, Michael (2004) *State of Fear*, HarperCollins Publishers India, New Delhi.
- [2] Etheridge, D. M., Steele, L. P., Langenfelds, R. L., Francey, R. J., Barnola, J. M., and Morgan, V. I. (1998) "Historical CO₂ records from the Law Dome DE08, DE08-2, and DSS ice cores," in *Trends: A Compendium of Data on Global Change*, CDIAC, ORNL, Oak Ridge, TN, USA.
<http://cdiac.ornl.gov/ftp/trends/co2/lawdome.combined.dat>
- [3] Gu, L., Baldocchi, D. D., Wofsy, S. C., Munger, J. W., Michalsky, J. J., Urbanski, S. P., and Boden, T. A. (2003) "Response of a deciduous forest to the Mount Pinatubo eruption: enhanced photosynthesis," *Science*, vol. 299, pp. 2035-2038.
<http://www.sciencemag.org/content/vol299/issue5615/index.shtml>
- [4] Inhofe, J. M. (2005) "Climate change update: Senate floor statement by U. S. Sen. James M. Inhofe (R-Okla)."
<http://inhofe.senate.gov/pressreleases/climateupdate.htm>
- [5] Jones, P. D., New, M., Parker, D. E., Martin, S., and Rigor, I. G. (1999) "Surface air temperature and its changes over the past 150 years," *Reviews of Geophysics*, vol. 37, pp. 173-199.

- [6] Jones, P. D. and Moberg, A. (2003) "Hemispheric and large-scale surface air temperature variations: An extensive revision and an update to 2001," *Journal of Climate*, vol. 16, pp. 206-223. <http://www.cru.uea.ac.uk/ftpdata/tavegl2v.dat>
- [7] Keeling, C. D. and Whorf, T. P. (2005) "Atmospheric CO₂ records from sites in the SIO air sampling network," in *Trends: A Compendium of Data on Global Change*, CDIAC, ORNL, Oak Ridge, TN, USA. <http://cdiac.ornl.gov/ftp/trends/co2/maunaloa.co2>
- [8] Marland, G., Boden, T. A. and Andres, R. J. (2005) "Global, regional, and national CO₂ emissions," in *Trends: A Compendium of Data on Global Change*. CDIAC, ORNL, Oak Ridge, TN, USA. http://cdiac.ornl.gov/ftp/ndp030/global.1751_2002.ems
- [9] Neftel, A., Friedli, H., Moor, E., Lötscher, H., Oeschger, H., Siegenthaler, U., and Stauffer, B. (1994) "Historical CO₂ record from the Siple Station ice core," in *Trends: A Compendium of Data on Global Change*, CDIAC, ORNL, Oak Ridge, TN, USA. <http://cdiac.ornl.gov/ftp/trends/co2/siple2.013>
- [10] Rust, B. W. (2001) "Fitting Nature's basic functions Part II: estimating uncertainties and testing hypotheses," *Computing in Science & Engineering*, vol. 3, pp. 60-64. <http://math.nist.gov/~BRust/Gallery.html>
- [11] Rust, B. W. (2003) "Fitting Nature's basic functions Part IV: the variable projection algorithm," *Computing in Science & Engineering*, vol. 5, pp. 74-79. <http://math.nist.gov/~BRust/Gallery.html>
- [12] Rust, B. W. (2003) "Separating signal from noise in global warming," *Computing Science and Statistics*, vol. 35, pp 263-277. <http://math.nist.gov/~BRust/Gallery.html>
- [13] Rust, B. W. and Kirk, B. L. (1982) "Modulation of fossil fuel production by global temperature variations," *Environment International*, vol. 7, pp. 419-422.
- [14] Schlesinger, M. E. and Ramankutty, N. (1994) "An oscillation in the global climate system of period 65-70 years," *Nature*, vol. 367, pp. 723-726.
- [15] Schmidt, Gavin (2004) "Michael Crichton's state of confusion," *Earth Institute News*, Columbia University, New York, Dec. 17, 2004. <http://www.earthinstitute.columbia.edu/news/2004/story12-13-04b.html>
- [16] Watts, J. A. (1982) "The carbon dioxide question: data sampler." in *Carbon Dioxide Review: 1982*, Clark, W. C., editor, Oxford University Press, New York, pp. 431-469
- [17] Will, George (2004) "Global warming? Hot air," *The Washington Post*, Thursday, Dec. 23, 2004, page A23. <http://www.washingtonpost.com/wp-dyn/articles/A20998-2004Dec22.html>